

## Detection of two massive CO systems in 4C 41.17 at $z = 3.8$

C. De Breuck<sup>1</sup>, D. Downes<sup>2</sup>, R. Neri<sup>2</sup>, W. van Breugel<sup>3</sup>, M. Reuland<sup>3,4</sup>, A. Omont<sup>5</sup>, and R. Ivison<sup>6,7</sup>

<sup>1</sup> European Southern Observatory, Karl Schwarzschild Straße 2, 85748 Garching, Germany  
e-mail: cdebrec@eso.org

<sup>2</sup> Institut de Radioastronomie Millimétrique, Domaine Universitaire, 38406 St. Martin-d'Hères, France  
e-mail: neri, downes@iram.fr

<sup>3</sup> IGPP/LLNL, L-413, 7000 East Ave, Livermore, CA 94550, USA  
e-mail: wil@igpp.ucllnl.org

<sup>4</sup> Sterrewacht Leiden, Postbus 9513, 2300 RA Leiden, The Netherlands  
e-mail: reuland@strw.leidenuniv.nl

<sup>5</sup> Institut d'Astrophysique de Paris, CNRS & Université Paris 6, 98bis Boulevard Arago, 75014 Paris, France  
e-mail: omont@iap.fr

<sup>6</sup> Astronomy Technology Centre, Royal Observatory, Blackford Hill, Edinburgh EH9 3HJ, UK

<sup>7</sup> Institute for Astronomy, University of Edinburgh, Royal Observatory, Blackford Hill, Edinburgh EH9 3HJ, UK  
e-mail: rji@roe.ac.uk

Received 20 October 2004 / Accepted 26 November 2004

**Abstract.** We have detected CO(4–3) in the  $z = 3.8$  radio galaxy 4C 41.17 with the IRAM Interferometer. The CO is in two massive ( $M_{\text{dyn}} \sim 6 \times 10^{10} M_{\odot}$ ) systems separated by  $1''.8$  (13 kpc), and by  $400 \text{ km s}^{-1}$  in velocity, which coincide with two different dark lanes in a deep Ly $\alpha$  image. One CO component coincides with the cm-radio core of the radio galaxy, and its redshift is close to that of the He II  $\lambda$  1640 AGN line. The second CO component is near the base of a cone-shaped region southwest of the nucleus, which resembles the emission-line cones seen in nearby AGN and starburst galaxies. The characteristics of the CO sources and their mm/submm dust continuum are similar to those found in ultraluminous IR galaxies and in some high- $z$  radio galaxies and quasars. The fact that 4C 41.17 contains two CO systems is further evidence for the role of mergers in the evolution of galaxies at high redshift.

**Key words.** galaxies: individual: 4C 41.17 – galaxies: active – galaxies: formation – radio lines: galaxies

### 1. Introduction

Because of its luminosity and large angular extent, 4C 41.17 has become the most studied high redshift radio galaxy (HzRG). *HST* images show that its host galaxy contains several star-forming components, including (i) a linear radio-aligned feature with spectroscopic characteristics of a young stellar population (Dey et al. 1997); (ii) a clumpy system, separate from the radio source, and (iii) low surface brightness UV emission extending over 70 kpc (van Breugel et al. 1999). The entire system is embedded in a giant Ly $\alpha$  halo (Reuland et al. 2003) and diffuse soft X-ray emission (Scharf et al. 2003). In spite of the detection of its dust emission (Dunlop et al. 1994; Chini & Krügel 1994), searches for molecular gas have been unsuccessful up to now (Ivison et al. 1996; Evans et al. 1996; Barvainis & Antonucci 1996; Scoville et al. 1996). In this letter, we report the first detection of two massive CO components near the centre of this large forming galaxy<sup>1</sup>.

<sup>1</sup> We adopt  $H_0 = 71 \text{ km s}^{-1} \text{ Mpc}^{-1}$ ,  $\Omega_M = 0.27$  and  $\Omega_{\Lambda} = 0.73$ . At  $z = 3.8$ , the luminosity distance  $D_L = 34.4 \text{ Gpc}$ , and  $1''$  corresponds to 7.2 kpc.

### 2. Observations and data reduction

We observed 4C 41.17 at 3.1 and 1.2 mm with the IRAM Plateau de Bure Interferometer in its compact *D* configuration between 1999 August and 2003 August. The spectral correlator covered a bandwidth of 580 MHz at each frequency. At 3.1 mm, the 6-antenna equivalent on-source observing time was 29 h, and the beam was  $7''.0 \times 4''.7$  at PA  $107^\circ$ . The central frequency was initially tuned to 96.090 GHz to observe CO(4–3) ( $\nu_{\text{rest}} = 461.040 \text{ GHz}$ , but later re-centred to 96.250 GHz to better cover the detected line. After phase and amplitude calibration, we merged the data at different centre frequencies into a data-set of 36 channels of 20 MHz each. As a result, the outer 7 channels on each end have  $\sigma \approx 0.9 \text{ mJy}$  compared to  $\sigma \approx 0.6 \text{ mJy}$  in the central ones. In the final data cube, the zero point of the velocity scale is 96.093 GHz, corresponding to  $z = 3.79786$ , the redshift of the He II  $\lambda$  1640 line (Dey et al. 1997). We made naturally weighted maps using the *AIPS* task *IMAGR*, with CLEANing applied only to the velocity-integrated maps.

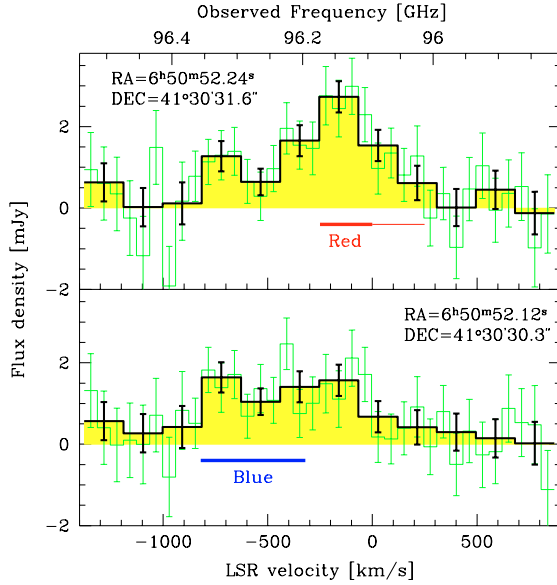


**Fig. 1.** CO (4–3) spectra at the positions of the red (top panel) and blue components (bottom). The thin green line shows the data in  $62 \text{ km s}^{-1}$  channels, and the thick black line in  $184 \text{ km s}^{-1}$  channels. Error bars are  $1\sigma$ , and velocities are relative to  $96.093 \text{ GHz}$  ( $z_{\text{LSR}} = 3.79786$ ). The red and blue bars indicate the linewidths; the thick part of the red bar marks channels used in Fig. 3, left. Note that these two positions are less than a beam size away, and are therefore not fully independent.

**Table 1.** Observed and derived parameters for CO(4–3) in 4C 41.17.

Parameter	Red component	Blue component	Total
RA(J2000) <sup>a</sup> (peak)	6 <sup>h</sup> 50 <sup>m</sup> 52 <sup>s</sup> .24	6 <sup>h</sup> 50 <sup>m</sup> 52 <sup>s</sup> .12	6 <sup>h</sup> 50 <sup>m</sup> 52 <sup>s</sup> .17
DEC(J2000) <sup>a</sup> (peak)	41°30′31″.6	41°30′30″.3	41°30′30″.9
$\int S_{\text{CO}} dV$ [Jy km s <sup>-1</sup> ]	1.2 ± 0.15	0.6 ± 0.15	1.8 ± 0.2
Central velocity <sup>b</sup> [km s <sup>-1</sup> ]	-130 ± 50	-550 ± 100	-285 ± 100
Velocity width [km s <sup>-1</sup> ]	500 ± 100	500 ± 150	1000 ± 150
$L'_{\text{CO}}(4-3)$ [K km s <sup>-1</sup> pc <sup>2</sup> ]	$4.4 \times 10^{10}$	$2.2 \times 10^{10}$	$6.7 \times 10^{10}$
$M(\text{H}_2)$ [ $M_{\odot}$ ]	$3.6 \times 10^{10}$	$1.8 \times 10^{10}$	$5.4 \times 10^{10}$

<sup>a</sup> Positional uncertainty 0′.03 in RA and 0′.3 in Dec.

<sup>b</sup> Relative to  $96.093 \text{ GHz}$  ( $z = 3.79786$ ).

We observed simultaneously at  $1.2 \text{ mm}$  ( $241.453 \text{ GHz}$  DSB) to study the dust continuum. We used only  $1.2 \text{ mm}$  data taken with a precipitable water vapour content  $< 3 \text{ mm}$ , which gave a usable on-source observing time of  $7.7 \text{ h}$ , and an rms noise of  $0.8 \text{ mJy/beam}$ . The  $1.2 \text{ mm}$  beam was  $2''.9 \times 1''.5$  at PA  $100^\circ$ , but we convolved the image with a  $3''.0 \times 3''.0$  Gaussian.

In 2004 March, we also observed the 4C 41.17 field at  $1.2 \text{ mm}$  ( $\sim 250 \text{ GHz}$ ) with the 117-element MPIfR Millimeter Bolometer array (MAMBO-2; Kreysa et al. 1998) at the IRAM 30 m telescope. The beam FWHM is  $10''.7$  with an array size of  $4'$ . We made eight on-the-fly maps, with 41 subscans of  $40 \text{ s}$  each, while chopping the secondary mirror in azimuth at  $2 \text{ Hz}$  by  $39$ ,  $42$ , or  $45''$ . We reduced the data using MOPSIC (Zylka 1998). The map covers  $3' \times 3'$  with an rms noise of  $0.8 \text{ mJy}$ .

### 3. Results

Figure 1 shows CO(4–3) spectra at two positions. No line emission is detected in the range  $-1550$  to  $-1000 \text{ km s}^{-1}$  and

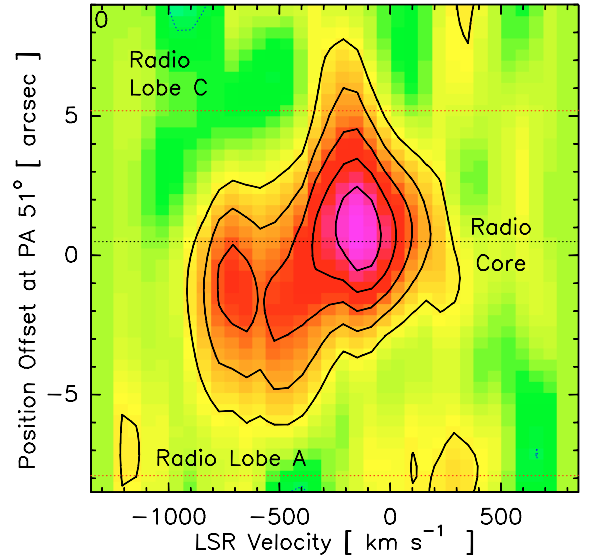


**Fig. 2.** CO (4–3) position-velocity slice at PA =  $51^\circ$  (i.e. along the radio axis). Horizontal lines mark the radio core and outer lobes. The position zero is  $6^{\text{h}}50^{\text{m}}52^{\text{s}}.17 \ 41^{\circ}30'30''.9$ , the beam along this cut is  $6''$ , and the contour steps are  $0.4 \text{ mJy}$ , with the first contour at  $0.4 \text{ mJy}$ .

$+250$  to  $+800 \text{ km s}^{-1}$  to  $0.75 \text{ mJy}$  ( $3\sigma$ ). In these outer channels, we find a marginal continuum emission at  $\sim 0.3 \text{ mJy}$ , which is consistent with the  $11 \text{ mJy}$  at  $850 \mu\text{m}$  (Ivison et al. 2000) and  $3.8 \text{ mJy}$  at  $1.2 \text{ mm}$  (our MAMBO map) extrapolated to  $3.1 \text{ mm}$  ( $\sim 0.2 \text{ mJy}$ ), and the non-thermal contribution of  $\lesssim 0.2 \text{ mJy}$  (over the  $13''$  source), extrapolated from  $6.4 \text{ mJy}$  at  $2 \text{ cm}$  (Chambers et al. 1990) and  $2.7 \text{ mJy}$  at  $1.2 \text{ cm}$  (Ivison et al. 1996). Because of these low values (below the first contour in Fig. 2), we do not correct the CO fluxes for the continuum.

The position-velocity slice (Fig. 2) shows that the CO emission has two components: (i) a “red” component at  $\sim -130 \text{ km s}^{-1}$  relative to  $z = 3.79786$ ; and (ii) a “blue” component at  $-550 \text{ km s}^{-1}$ . Figure 3 shows the integrated red and blue components<sup>2</sup>, separated by  $1''.8$  ( $13 \text{ kpc}$  projected). Table 1 lists the observed parameters, the line luminosity  $L'_{\text{CO}}(4-3)$ , and the molecular gas mass  $M(\text{H}_2)$ , calculated assuming a constant brightness temperature from CO(4–3) to CO(1–0) and a conversion factor  $X_{\text{CO}} = 0.8 M_{\odot} (\text{K km s}^{-1} \text{ pc}^2)^{-1}$  derived for local ultraluminous infrared galaxies (Downes & Solomon 1998).

Figure 4 shows three maps of the dust continuum in 4C 41.17. Unlike the solid  $10\sigma$  and  $5\sigma$  detections in the  $850 \mu\text{m}$  SCUBA and  $1.2 \text{ mm}$  MAMBO maps, our  $1.2 \text{ mm}$  interferometer map shows a  $4.3\sigma$  peak at  $06^{\text{h}}50^{\text{m}}52^{\text{s}}.24$ ,  $+41^{\circ}30'31''.9$  (J2000; i.e. at the red CO component) only after convolution with a  $3''.0$  Gaussian. This PdBI map yields a flux  $S_{1.2 \text{ mm}} = 3.0 \pm 0.7 \text{ mJy}$ , consistent with the  $S_{1.2 \text{ mm}} = 3.8 \pm 0.6 \text{ mJy}$  from the MAMBO map. The S/N in our  $1.2 \text{ mm}$  maps is insufficient to constrain the spatial extent of the thermal dust emission reported by Ivison et al. (2000) and Stevens et al. (2003).

Both CO components are gas-rich systems with  $M_{\text{H}_2} \sim 3 \times 10^{10} M_{\odot}$  (Table 1). Their projected separation of  $13 \text{ kpc}$  and apparent relative velocity of  $\sim 400 \text{ km s}^{-1}$  imply a combined

<sup>2</sup> To increase S/N, the red component in Fig. 3 covers only the brightest  $250 \text{ km s}^{-1}$ , indicated by the thick bar in Fig. 1 (top).

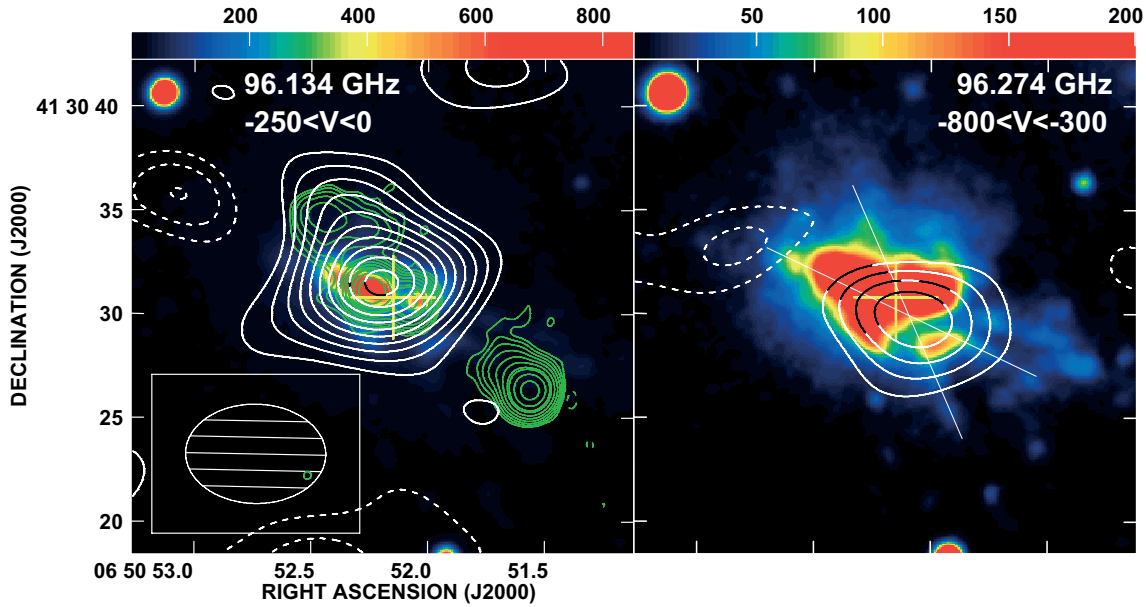


**Fig. 3.** Velocity-averaged CO maps (thick/white+black contours) of the red (*left*) and blue (*right*) components. CO contours are  $-3, -2, 2, 3, \dots, 10\sigma$ , with  $\sigma = 0.2 \text{ mJy beam}^{-1}$ . The lower left inset shows the CO beam. The two CO maps are superposed on the  $\text{Ly}\alpha$  image, each with its own colour scheme to show the two dark lanes in the  $\text{Ly}\alpha$ . The thin green contours (*left panel*) show the 1.4 GHz radio map (Carilli et al. 1994), and the yellow cross indicates the radio core. The thin straight lines (*right panel*) indicate a possible AGN or starburst emission-line cone.

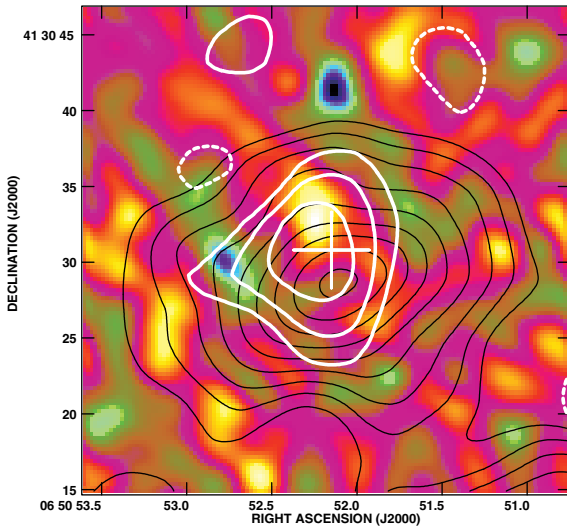


**Fig. 4.** Thermal dust emission in 4C 41.17. The colourscale shows the 1.2 mm PdBI map convolved with a  $3''$  Gaussian (not corrected for the  $20''$  primary beam). Superposed are the  $850 \mu\text{m}$  SCUBA map (thin black contours; beam  $14''$ ) and our 1.2 mm MAMBO map (thick white contours; beam  $11''$ ). Contours are  $-2, 2, 3, 4, 5, 6, 7, 8, 9$  and  $10\sigma$ , with  $\sigma = 1.2$  and  $0.8 \text{ mJy beam}^{-1}$  for the SCUBA and MAMBO maps, respectively. The white cross indicates the cm-radio core.

dynamical mass  $R\Delta V^2/G$  of  $\gtrsim 6 \times 10^{10} M_{\odot}$ , an order of magnitude smaller than the typical baryonic mass of HzRGs integrated over 64 kpc (Rocca-Volmerange et al. 2004).

We associate the red CO component with the AGN because:

(i) it agrees within the uncertainties, with the cm-radio core position (Carilli et al. 1994) and the hard X-ray point source (Scharf et al. 2003); (ii) it coincides with the central dark lane

seen in the  $\text{Ly}\alpha$  image (Fig. 3, *left*, near the cross) and the HST  $R$ -band image (Bicknell et al. 2000); and (iii) it has the same velocity offset as the low-ionization interstellar absorption lines in the deep Keck spectrum of Dey et al. (1997). The CO redshift of  $3.7958 \pm 0.0008$  is thus likely to be the real systemic redshift of the host galaxy of 4C 41.17.

The blue CO component peaks at the position of a second apparent dark lane in the  $\text{Ly}\alpha$  image (Fig. 3, *right*), which suggests that the  $\text{Ly}\alpha$  may be absorbed by dust of another kinematic system, associated with this CO. This apparent  $\text{Ly}\alpha$  absorption lane is in a region which resembles the emission-line cones seen, although on smaller scales (a few kpc), in some nearby AGN (e.g. Cygnus A; Canalizo et al. 2003) as well as in starburst galaxies (e.g. Veilleux & Rupke 2002).

#### 4. Discussion and conclusions

What is the relation between the molecular CO-gas, the dust, the  $\text{Ly}\alpha$  halo, and the massive forming galaxy with its radio-loud AGN? Our CO velocity profile (Fig. 2) shows a remarkable similarity to the  $\text{Ly}\alpha$  velocity profile of Dey (1999). Both the CO and  $\text{Ly}\alpha$  are split into two components, separated by a projected distance of  $\sim 13 \text{ kpc}$ , and by  $\sim 400 \text{ km s}^{-1}$ . This suggests that the  $\text{Ly}\alpha$  emission may also come from two separate components (rather than a single component split by an associated HI absorber). However,  $\text{Ly}\alpha$  traces much less dense gas ( $n_{\text{H}} \sim 17\text{--}150 \text{ cm}^{-3}$ ; Villar-Martín et al. 2003) than CO, which must have a density of  $10^3$  to  $10^4 \text{ cm}^{-3}$  to have enough CO-line opacity to give a typical brightness temperature of order 30 K. Hence, the CO and  $\text{Ly}\alpha$  may originate from the same gas-rich systems, but they do not necessarily trace the total extent of these regions. This is obvious from the 200 kpc spatial extent

of the Ly $\alpha$ , while the CO emission is unresolved with our 6'' (43 kpc) beam. In fact, we can put even stronger constraints on the size of the CO-line sources, using some basic assumptions.

The FIR dust luminosity of 4C 41.17 is very high,  $L_{\text{FIR}} \approx 1.5 \times 10^{13} L_{\odot}$ , a value typical of an ultraluminous starburst. The FIR fluxes, including our new continuum data points at 3.1 and 1.2 mm, imply a dust temperature of  $54 \pm 10$  K, in agreement with earlier values (Benford et al. 1999; Scharf et al. 2003). Although the mm/sub-mm continuum is optically thin, the CO lines are not, so the observed brightness temperature of the CO will be about the same as the gas temperature. The existing interferometer CO maps of ULIRGs, the only nearby objects with comparable FIR luminosity, show that the brightness temperatures of the low- $J$  CO lines are comparable with the FIR dust temperature (Downes & Solomon 1998). Indeed, for high- $z$  CO detections even to be possible, the gas must have a significant brightness temperature, typically 30 to 50 K, over several hundred pc. For 4C 41.17, this means that if the CO(4–3) brightness temperature is  $\sim 30$  K, then the observed CO(4–3) luminosity (Table 1) implies a CO source diameter  $d = (4 L'_{\text{CO}} / (\pi T_{\text{b}} \Delta V))^{0.5}$  of 1.4 to 1.8 kpc, or 0''.2 to 0''.25.

This size and H<sub>2</sub> mass imply a hydrogen column density of order  $10^{24} \text{ cm}^{-2}$ , which is consistent with the observed mm-FIR dust spectrum becoming opaque near restframe 100  $\mu\text{m}$ . Applying the Stefan-Boltzmann formula with the derived CO source diameter  $d \sim 1.6$  kpc and dust temperature then yields  $L_{\text{FIR}} = \pi \sigma d^2 T^4 \approx 10^{13} L_{\odot}$ , similar to the observed value. The CO source size is also roughly consistent with the total mass and typical density of the CO gas ( $10^3$  to  $10^4 \text{ cm}^{-3}$ ), which imply source sizes of order  $\sim 1$  kpc, depending on geometry. Note that these are maximum sizes of the CO. If one assumes the CO is in more than two sources, then each component will have a smaller size. We also note that our observations are insensitive to more widely distributed, cooler CO.

The only known place where such high gas densities over such dimensions are found are the circumnuclear disks observed in ULIRGs and some quasars. The “red” CO source in 4C 41.17 thus finds a natural interpretation as a circumnuclear starforming disk around the radio-loud AGN. The fact that there appears to be a second such CO source, 13 kpc away, separated by  $\sim 400 \text{ km s}^{-1}$  in velocity, that also contains about the same mass of molecular gas, suggests the AGN and possibly starburst activity may have been triggered by the interaction of the two objects. The absence of UV/optical continuum signatures of starburst activity at the position of the blue CO component remains surprising. A possible explanation could be that this starburst has not yet reached its peak UV/optical emission (Haas et al. 2003).

To summarize: our observations indicate that the 4C 41.17 system contains two massive CO components, each of which may be associated with an obscured black hole. This is remarkably similar to the two CO systems in 4C 60.07 (Papadopoulos et al. 2000; Greve et al. 2004). There are three other HzRGs, 6C 1909+72, B3 J2330+3927 and TN J0120+1320 with detected CO (Papadopoulos et al. 2000; De Breuck et al. 2003a,b). It will be of interest to determine if they are also

double sources in CO, which would further indicate the role of mergers in triggering AGN activity in the most massive galaxies at high redshift.

*Acknowledgements.* IRAM is supported by INSU/CNRS (France), MPG (Germany) and IGN (Spain). The work by W.v.B. and M.R. was performed at IGPP/LLNL under the auspices of the US Department of Energy, National Nuclear Security Administration by the University of California, Lawrence Livermore National Laboratory under contract No. W-7405-Eng-48. This work was carried out in the context of EARA, the European Association for Research in Astronomy.

## References

- Barvainis, R., & Antonucci, R. 1996, *PASP*, 108, 187  
 Benford, D., Cox, P., Omont, A., Phillips, T., & McMahon, R. 1999, *ApJ*, 518, L65  
 Bicknell, G., Sutherland, R., van Breugel, W., et al. 2000, *ApJ*, 540, 678  
 Canalizo, G., Max, C., Whysong, D., Antonucci, R., & Dahm, S. 2003, *ApJ*, 597, 823  
 Carilli, C., Owen, F., & Harris, D. 1994, *AJ*, 107, 480  
 Chambers, K., Miley, G., & van Breugel, W. 1990, *ApJ*, 363, 21  
 Chini, R., & Krügel, E. 1994, *A&A*, 288, L33  
 De Breuck, C., Neri, R., Morganti, R., et al. 2003a, *A&A*, 401, 911  
 De Breuck, C., Neri, R., & Omont, A. 2003b, *New Astron. Rev.*, 47, 285  
 Dey, A., van Breugel, W., Vacca, W., & Antonucci, R. 1997, *ApJ*, 490, 698  
 Dey, A. 1999, *The Hy-Redshift Universe: Galaxy Formation and Evolution at High Redshift*, ed. A. J. Bunker, & W. J. M. van Breugel (San Francisco: ASP), ASP Conf. Ser., 193, 34  
 Downes, D., & Solomon, P. 1998, *ApJ*, 507, 615  
 Dunlop, J., Hughes, D., Rawlings, S., Eales, S., & Ward, M. 1994, *Nature*, 370, 347  
 Evans, A., Sanders, D. B., Mazzarella, J. M., et al. 1996, *ApJ*, 457, 658  
 Greve, T., Ivison, R., & Papadopoulos, P. 2004, *A&A*, 419, 99  
 Haas, M., Klaas, U., Müller, S. A. H., et al. 2003, *A&A*, 402, 87  
 Ivison, R., Papadopoulos, P., Seaquist, E., & Eales, S. 1996, *MNRAS*, 278, 669  
 Ivison, R., Dunlop, J., Smail, I., et al. 2000, *ApJ*, 542, 27  
 Kreysa, E., Gemuend, H.-P., Gromke, J., et al. 1998, *Proc. SPIE*, 3357, 319  
 Papadopoulos, P., Röttgering, H. J. A., van der Werf, P. P., et al. 2000, *ApJ*, 528, 626  
 Reuland, M., van Breugel, W., Röttgering, H., et al. 2003, *ApJ*, 592, 755  
 Rocca-Volmerange, B., Le Borgne, D., De Breuck, C., Fioc, M., & Moy, E. 2004, *A&A*, 415, 931  
 Scharf, C., Smail, I., Ivison, R., et al. 2003, *ApJ*, 596, 105  
 Scoville, N., Yun, M., & Bryant, P. 1996, *Cold Gas at High Redshift*, ed. M. N. Bremer, et al. (Dordrecht: Kluwer), *ASSL*, 206, 25  
 Stevens, J., Ivison, R. J., Dunlop, J. S., et al. 2003, *Nature*, 425, 264  
 van Breugel, W., et al. 1999, in *The Most Distant Radio Galaxies*, ed. H. J. A. Röttgering, P. N. Best, & M. D. Lehnert (Amsterdam: Roy. Neth. Acad. Sci.), 49  
 Veilleux, S., & Rupke, D. 2002, *ApJ*, 565, L63  
 Villar-Martín, M., Vernet, J., di Serego Alighieri, S., et al. 2003, *MNRAS*, 346, 273  
 Zylka, R., *The MOPSI Cookbook*, IRAM